IEEE Access
Multidisciplinary | Rapid Review | Open Access Journal

Received April 23, 2018, accepted May 19, 2018, date of publication May 24, 2018, date of current version June 29, 2018.

Digital Object Identifier 10.1109/ACCESS.2018.2840155

Omission Error Analysis in Gravity Gradient Measurement

HONGWEI WEI, MEIPING WU, JULIANG CAO, JUNXIANG LIAN, AND SHAOKUN CAI
College of Intelligent Science and Technology, National University of Defense Technology, Changsha 410073, China

Corresponding authors: Hongwei Wei (weihongweier@nudt.edu.cn) and Meiping Wu (meipingwu@263.net)

This work was supported in part by the National Key R&D Program of China under Grant 2017YFC0601701 and in part by the National Natural Science Foundation of China under Grant 61603401 and Grant 61273055.

ABSTRACT Gravity gradient plays an important role in many fields of science, and many methods are used to achieve the measurement of it. To improve measurement accuracy, various error analyses have been conducted in previous studies about positioning and orientation errors and system noise, among others. However, knowledge on the influence of omission errors from the theoretical models of gravity gradient measurement is limited. In this paper, we investigated omission errors in gravity gradient measurement, which was accomplished with the principle of differential acceleration. First, we determined the source of the omission errors to be the omission of high-order terms. Second, we calculated these terms on the basis of the Earth Gravitational Model 2008. Specifically, the expression of the partial derivative of the high order for the gravity potential in the spherical coordinates and the recursive equations for the high-order partial derivatives of the Legendre function were derived. Moreover, we transformed these high-order terms from the spherical coordinate system to the local north-oriented frame. The analysis led to three findings. First, a positive correlation was found between the omission errors and the distance between two measuring points. Second, the influences of the omission errors varied across different regions. Third, Γ_{zz} was the least affected by the omission errors among the components Γ_{xz}, Γ_{yz}, and Γ_{zz}. In conclusion, our study demonstrates that omission errors affect gravity gradient measurement.

INDEX TERMS EGM2008, gravity gradient, omission error.

I. INTRODUCTION

Gravity gradient $\mathbf{\Gamma}$, as the second spatial derivative of the Earth's geopotential [1], can be measured directly to estimate the gravitational field, which is important in the development of many disciplines.

Compared with the measurement of the first spatial derivative of the Earth's geopotential V, which is the gravity $\mathbf{g}$, gravity gradient can deliver more detailed and accurate information about the underlying geological setting in geological prospection [2] because the gravity gradient can be composed of more components simultaneously. Moreover, the use of gravity gradient can overcome limitations in spatial resolution and accuracy that are inherent in ordinary moving-base gravimetry [3]. With the abovementioned advantages, gravity gradient signal is widely used in various fields of technology to locate submerged objects [4], [5], explore minerals and hydrocarbons [6], [7], and target compact, local, subterranean voids [8]. The gravity gradient signal is also used to assist in inertial navigation. With the support of gravity gradient signal, the positioning accuracy of inertial navigation can be increased by several hundred meters per hour [9]–[14].

The gravity gradient signal is weak, and even small errors in gravity gradient measurement considerably affect measurement results. Various error sources in gravity gradient measurement have been analyzed in previous studies to improve the accuracy of the measurement [15], [16]. Fuchs, M. J. investigated the projection of the errors caused by a rotation from the gradiometer reference frame to local reference frames and concluded that these errors can be compensated by replacing the insignificantly accurate gravity gradients with model values [17]. For the effect of attitude reconstitution errors, Pail [18] studied these errors by numerical simulations and proved that these errors represent a substantial error component of the gravity field solution. Li *et al.* [19] analyzed the influences of satellite positioning errors and Earth's multipole moments on the measurement of gravity gradient . Random and systematic errors in such measurement have also been studied [20], [21]. Bouman *et al.* [20] found that with the existing global models, it is possible to

remove a large part of the systematic errors of the Gravity Field and Steady-State Ocean Circulation Explorer gradients. And gravity gradient bias can be accurately recovered on the basis of terrestrial gravity data and be compensated. Wang *et al.* [21] discussed the systematic error of differential phase measurement in gravity gradient measurement by using dual-atom interferometers and showed that systematic errors largely decrease with a symmetrical modulation of the magnetic field duration . Other errors, such as those caused by misalignments between star sensor and gradiometer [22], instrument errors [3], and tidal and nontidal corrections [23], have also been studied. The aforementioned analysis results imply that the influences of many error sources can be compensated and the accuracy of gravity gradient measurement has been improved significantly.

However, theoretical measurement errors cannot be eliminated by error compensation, and they have only rarely been investigated in previous research. Theoretical errors are model errors in measurement, and they remain in the measurement results even with a perfect measurement environment and devices. The study of the theoretical errors in the gravity gradient measurement will help to increase our understanding of the gravity gradient and make better use of the gravity gradient data. In this study, we investigate how theoretical errors influence gravity gradient measurement.

The contributions of this study are as follows.

1) The origin of theoretical errors is determined through the basic principle of gravity gradient measurement.
2) Calculation formulas for the theoretical errors are derived.
3) A simulation test for the theoretical errors is conducted.
4) The influences of the theoretical errors on the different components of a gravity gradient tensor are discussed.

II. BASIC PRINCIPLE OF GRAVITY GRADIENT MEASUREMENT

Many gravity gradient measurement methods based on different principles have been proposed. For example, Moody *et al.* [24]. measured the diagonal components of the gravity gradient tensor using superconducting technology. McGuirk *et al.* [25] improved an absolute-gravity gradiometer by light-pulse atom interference techniques. Douch *et al.* [6], [7] proposed GREMLIT, a gravity gradiometer concept that comprises a planar acceleration gradiometer and three gyroscopes. Similarly, Araya *et al.* developed a gravity gradiometer that consists of two vertically separated accelerometers; their motions can be precisely detected by optical sensors. A gravity gradient measure system based on rotating accelerometers, which was developed for submarine applications, has also been widely used for exploration [27]. All of these methods obtain gravity gradient signal by the differential acceleration principle. This principle can be simplified as shown in Figure 1, where o–xyz is a Cartesian coordinate system, and A, B, C, and D are points in the space.

The gravity vectors at the four positions (A, B, C, and D) are denoted by $\mathbf{g}_p$ ($p \in \{A, B, C, D\}$), which comprises three components, namely,

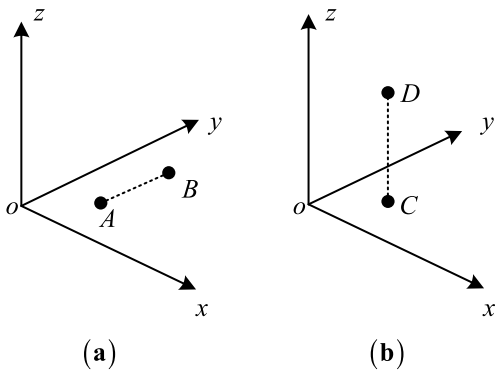

FIGURE 1. Measurement principle of gravity gradiometer based on differential acceleration. In Figure 1(a), A and B lie on the x–o–y plane and the line between A and B is parallel to the y-axis. In Figure 1(b), C and D are on the x–o–z plane and the line between C and D is parallel to the z-axis. The distance between A and B is denoted by l_{AB}, and the distance between C and D is denoted by l_{CD}.

$$\mathbf{g}_p = \left(g_{xp}, g_{yp}, g_{zp}\right)', \tag{1}$$

where g_{xp}, g_{yp}, and g_{zp} represent the projection of gravity vector $\mathbf{g}_p$ in the x, y, and z directions, respectively.

The measurement models of gravity gradient at the midpoint of l_{AB} and l_{CD} are as follows:

$$\begin{aligned}
\Gamma_{xy} &= \frac{(g_{xB} - g_{xA})}{l_{AB}} \\
\Gamma_{yy} &= \frac{\left(g_{yB} - g_{yA}\right)}{l_{AB}} \\
\Gamma_{zy} &= \frac{(g_{zB} - g_{zA})}{l_{AB}} \\
\Gamma_{xz} &= \frac{(g_{xD} - g_{xC})}{l_{CD}} \\
\Gamma_{yz} &= \frac{\left(g_{yD} - g_{yC}\right)}{l_{CD}} \\
\Gamma_{zz} &= \frac{(g_{zD} - g_{zC})}{l_{CD}},
\end{aligned} \tag{2}$$

where Γ_{xy}, Γ_{yy}, Γ_{zy}, Γ_{xz}, Γ_{yz}, and Γ_{zz} are the different components of the gravity gradient tensor.

Does any error exist? In other words, does any difference exist between the theoretical value and the signal measured by this measurement model? Yes. But the omission error can be ignored when the baseline is small, and we will explain this in detail.

Zheleznyak *et al.* [28] measured vertical gravity gradient. The measured value of this gradient according to Equation (2) is 2201 E ($1E = 10^{-9}s^{-2}$), but the theoretical prediction of the vertical gravity gradient Γ_{zz} is 2222.14 E. Therefore, the measured and theoretical values differ. This difference may be caused by measurement and theoretical errors, and the extent to which these theoretical errors affect the measurement is unknown. Thus, we focus on analyzing theoretical errors in the following part.

III. OMISSION ERRORS AND THEIR CALCULATION

Geopotential contains all the information about the gravity field. As an approximation to geopotential, the Earth Gravitational Model 2008 (EGM2008) contains almost all information about the gravity field.

A. OMISSION ERRORS IN GRAVITY GRADIENT MEASUREMENT

Theoretical errors are generated in measuring gravity gradient using Equation (2) mainly due to omitting high-order terms. Thus, the theoretical errors in this study are labeled omission errors. The following step regards points A and B in Figure 1 (a) as examples to deduce the expression of the omission errors.

The Taylor expansion of gravity vector indicates that the gravity vector $\mathbf{g}_B$ at point B and the gravity vector $\mathbf{g}_A$ at point A are related; that is,

$$g_{iB} = g_{iA} + \frac{\partial g_{iA}}{\partial y} l_{AB} + \frac{1}{2!}\frac{\partial^2 g_{iA}}{\partial y^2} l_{AB}^2 + \frac{1}{3!}\frac{\partial^3 g_{iA}}{\partial y^3} l_{AB}^3 + \cdots (i \in \{x, y, z\}), \quad (3)$$

where $\frac{\partial g_{iA}}{\partial y} = \Gamma_{iy}\ (i \in \{x, y, z\})$.

The gravity gradient component is obtained as

$$\Gamma_{iy} = \frac{(g_{iB} - g_{iA}) - \left(\frac{1}{2!}\frac{\partial^2 g_{iA}}{\partial y^2} l_{AB}^2 + \frac{1}{3!}\frac{\partial^3 g_{iA}}{\partial y^3} l_{AB}^3 + \cdots\right)}{l_{AB}}. \quad (4)$$

A comparison of Equations (2) and (5) shows that the omission error $\delta\Gamma_{iy}$ in the gravity gradient measurement, which is generated by using the differential acceleration method, is

$$\delta\Gamma_{iy} = \frac{1}{2!}\frac{\partial^2 g_{iA}}{\partial y^2} l_{AB} + \frac{1}{3!}\frac{\partial^3 g_{iA}}{\partial y^3} l_{AB}^2 + \cdots. \quad (5)$$

In the same way, when the gravity gradient measurement is performed at measuring points C and D, as shown in Figure 1 (b), the omission error $\delta\Gamma_{iz}$ is

$$\delta\Gamma_{iz} = \frac{1}{2!}\frac{\partial^2 g_{iC}}{\partial z^2} l_{CD} + \frac{1}{3!}\frac{\partial^3 g_{iC}}{\partial z^3} l_{CD}^2 + \cdots \quad (6)$$

When measuring the gravity gradient component Γ_{ix} at measuring points E and F, as shown in Figure 2, the omission error $\delta\Gamma_{ix}$ is

$$\delta\Gamma_{ix} = \frac{1}{2!}\frac{\partial^2 g_{iE}}{\partial x^2} l_{EF} + \frac{1}{3!}\frac{\partial^3 g_{iE}}{\partial x^3} l_{EF}^2 + \cdots. \quad (7)$$

To calculate the omission error, the following terms need to be calculated:

$$\begin{aligned} &\frac{\partial^n g_{iA}}{\partial y^n}\ (i \in \{x, y, z\}, n = 2, 3, ...) \\ &\frac{\partial^n g_{iC}}{\partial z^n}\ (i \in \{x, y, z\}, n = 2, 3, ...) \\ &\frac{\partial^n g_{iE}}{\partial x^n}\ (i \in \{x, y, z\}, n = 2, 3, ...). \end{aligned} \quad (8)$$

Reference [29] showed that the relationship between geopotential and components of the gravity vector is as follows

$$g_i = \frac{\partial V(x, y, z)}{\partial i}\ (i \in \{x, y, z\}). \quad (9)$$

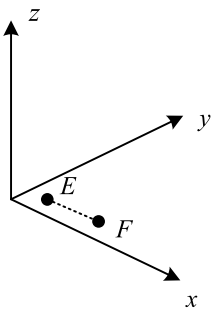

FIGURE 2. Schematic of measuring points E and F.

Equation (8) and (9) are substituted into Equations (5)–(7), and the omission error values are obtained.

The expressions for the omitted high-order terms are in the Appendix.

B. CALCULATION OF OMISSION ERRORS

The Earth's external gravitational potential V, at a point P defined in the Earth-fixed reference frame (EFRF) is given by [30] and [31]

$$V(r, \theta, \lambda) = \frac{GM}{r}\left[1 + \sum_{n=2}^{N\max}\left(\frac{a}{r}\right)^n \sum_{m=0}^{n}\left(\begin{matrix}\bar{C}_{nm}\cos m\lambda \\ +\bar{S}_{nm}\sin m\lambda\end{matrix}\right)\bar{P}_{nm}(\cos\theta)\right] \quad (10)$$

where GM is the geocentric gravitational constant. The value of a is the equatorial radius of the reference ellipsoid. r is the geocentric distance, θ is the geocentric colatitude, and λ is the longitude. $\bar{P}_{nm}(\cos\theta)$ is the fully normalized associated Legendre function. $\bar{C}_{nm}$ and $\bar{S}_{nm}$ are fully normalized spherical harmonic coefficients, which are given by EGM2008.

1) REFERENCE FRAME

A comparison of Equations (9) and (10) implies that their reference frames differ. The gravitational potential in Equation (9) is represented in the local north-oriented frame (LNOF), whereas that in Equation (10) is represented in the EFRF. Schematic of LNOF and EFRF are shown in Figure 3.

In Figure 3, the EFRF is the same as the World Geodetic System 1984 (WGS-84), with the coordinate origin located at the Earth's mass center. The LNOF is a local geographic frame; its origin is at the measurement location point o_L, and its axes align with the directions of north, east, and local vertical (down) [32]. The coordinates of point o_L in the EFRF are $(r_o, \theta_o, \lambda_o)$.

Calculating the derivatives of gravitational potential in the spherical coordinate system according to Equation (10) is convenient. Therefore, we first calculate the derivatives of the gravitational potential on the basis of spherical coordinates and then transfer the calculation results to the LNOF.

Figure 4 illustrates that to realize the transformation from spherical coordinates to the LNOF, the first step is to transfer

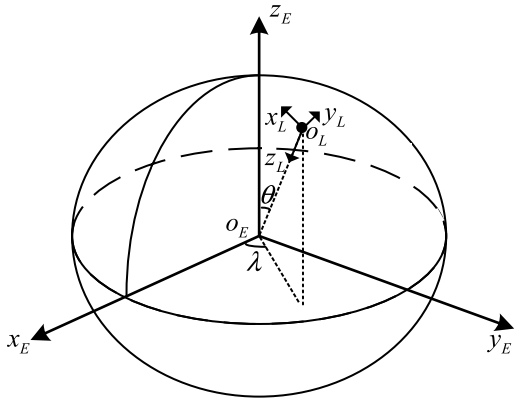

FIGURE 3. Schematics of LNOF and EFRF.

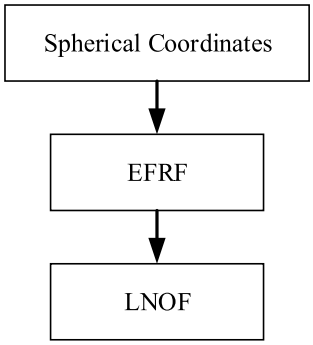

FIGURE 4. Flowchart of transformation from spherical coordinates to LNOF.

the computed results in the spherical coordinate system to the EFRF by

$$\begin{cases} \dfrac{\partial}{\partial x_E} = \dfrac{\partial r}{\partial x_E}\dfrac{\partial}{\partial r} + \dfrac{\partial \theta}{\partial x_E}\dfrac{\partial}{\partial \theta} + \dfrac{\partial \lambda}{\partial x_E}\dfrac{\partial}{\partial \lambda} \\ \dfrac{\partial}{\partial y_E} = \dfrac{\partial r}{\partial y_E}\dfrac{\partial}{\partial r} + \dfrac{\partial \theta}{\partial y_E}\dfrac{\partial}{\partial \theta} + \dfrac{\partial \lambda}{\partial y_E}\dfrac{\partial}{\partial \lambda} \\ \dfrac{\partial}{\partial z_E} = \dfrac{\partial r}{\partial z_E}\dfrac{\partial}{\partial r} + \dfrac{\partial \theta}{\partial z_E}\dfrac{\partial}{\partial \theta} + \dfrac{\partial \lambda}{\partial z_E}\dfrac{\partial}{\partial \lambda} \end{cases} \tag{11}$$

where

$$\begin{cases} x_E = r\sin\theta\cos\lambda \\ y_E = r\sin\theta\sin\lambda \\ z_E = r\cos\theta. \end{cases} \tag{12}$$

The transformation from EFRF to LNOF can be realized by the following Equations:

$$(x_L, y_L, z_L)' = C\,(x_E, y_E, z_E)', \tag{13}$$

where

$$C = \begin{pmatrix} -\sin\theta_o\cos\lambda_o & -\sin\theta_o\sin\lambda_o & \cos\theta_o \\ -\sin\lambda_o & \cos\lambda_o & 0 \\ -\cos\theta_o\cos\lambda_o & -\cos\theta_o\sin\lambda_o & -\sin\theta_o \end{pmatrix}. \tag{14}$$

TABLE 1. Simulation settings.

Variable	Values
GM	3.986004418×1014 m^3/s^2
a	6378137.00 m
f	1/298.257223563
h	0 m
d	0.4, 10, and 100 m
Maximum degree and order	2160

GM is the product of the Earth's mass and the gravitational constant; a is the semi-major axis of the WGS 84 ellipsoid, f is the flattening of the WGS 84 ellipsoid, h is the height of the measurement points from the reference ellipsoid, and d represents the distance between two points where accelerations are measured.

2) RECURRENCE EQUATIONS FOR DERIVATIVES OF FULLY NORMALIZED ASSOCIATED LEGENDRE FUNCTIONS

The preceding analysis indicates that the derivatives of the Legendre function are necessary in calculating the partial derivatives of the gravitational potential, such as V_{rrrr}, $V_{rr\theta\theta}$, and $V_{rr\lambda\lambda}$.

The recursive equations for the derivatives of the Legendre function are as follows. The recursion formulas of the first- and second-order partial derivatives were given in [33]. The recursion formulas of the third- and fourth-order partial derivatives of the Legendre polynomials are derived from the definition of the Legendre polynomials.

1) Initial values

$$\begin{aligned} \bar{P}_{00}(\cos\theta) &= 1 \\ \bar{P}_{10}(\cos\theta) &= \sqrt{3}\cos\theta \\ \bar{P}_{11}(\cos\theta) &= \sqrt{3}\sin\theta \end{aligned} \tag{15}$$

2) Recurrence formulas of $\bar{P}_{ij}(\cos\theta)$

$$\bar{P}_{n,m}(\cos\theta) = \begin{cases} 1, n = 0 \\ \sqrt{3}\sin\theta, n = 1 \\ \sqrt{\dfrac{2n+1}{2n}}\sin\theta\bar{P}_{n-1,m-1}(\cos\theta) \end{cases} \quad (n = m) \tag{16}$$

$$\begin{aligned} &\bar{P}_{n+1,m}(\cos\theta) \\ &= \sqrt{\frac{(2n+1)(2n+3)}{(n+m+1)(n-m+1)}}\cos\theta\bar{P}_{n,m}(\cos\theta) \\ &\quad - \sqrt{\frac{(2n+3)(n+m)(n-m)}{(2n-1)(n+m+1)(n-m+1)}} \\ &\quad \times \bar{P}_{n-1,m}(\cos\theta) \quad (n \neq m) \end{aligned} \tag{17}$$

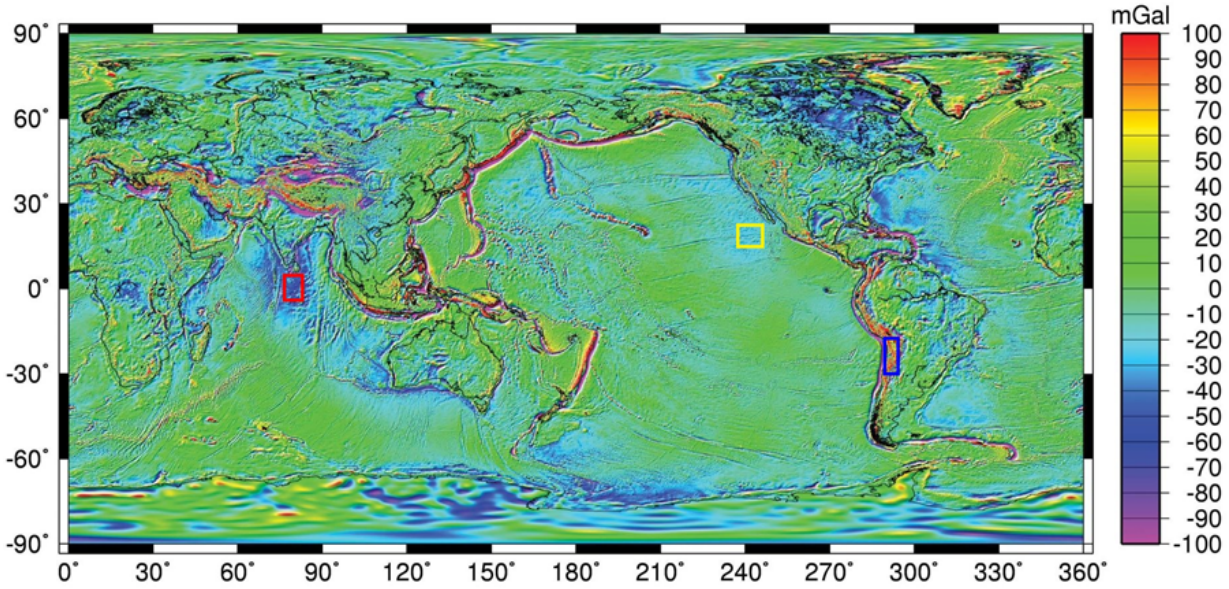

FIGURE 5. Regions for simulation: the areas in the red, yellow, and blue boxes, which are denoted as *A*, *B*, and *C*, have gravity anomalies of less than −30 mGal, between −20 and 10 mGal, and greater than 70 mGal, respectively.

TABLE 2. Coordinates of simulation regions.

Region	Longitude	Latitude
A	76° E–81° E	4° S –5° N
B	113° W–119° W	17° N–23° N
C	66° W–69° W	19° S–26° S

TABLE 3. Mean values of Γ_{xz}, Γ_{yz}, and Γ_{zz} calculated by EGM2008.

Region	Γxz	Γyz	Γzz	Unit
A	−0.5460666	0.3206101	3081.3812428	E
B	−9.1719462	0.2129704	3082.1387013	E
C	9.8820311	−0.0038620	3085.3528434	E

3) Recurrence formula of $\bar{P}'_{ij}(\cos\theta)$

$$\bar{P}'_{n,m}(\cos\theta) = \begin{cases} -\sqrt{\dfrac{n(n+1)}{2}}\bar{P}_{n,1}(\cos\theta) & (m=0) \\ \sqrt{\dfrac{n(n+1)}{2}}\bar{P}_{n,0}(\cos\theta) & \\ -\dfrac{\sqrt{(n-1)(n+2)}}{2}\bar{P}_{n,2}(\cos\theta) & (m=1) \\ -\dfrac{\sqrt{(n-m)(n+m+1)}}{2}\bar{P}_{n,m+1}(\cos\theta) & \\ +\dfrac{\sqrt{(n+m)(n-m+1)}}{2}\bar{P}_{n,m-1}(\cos\theta) & (n\neq m) \\ \sqrt{\frac{n}{2}}\bar{P}_{n,m-1}(\cos\theta) & (m=n) \end{cases} \tag{18}$$

4) Recurrence formula of $\bar{P}''_{ij}(\cos\theta)$

$$\bar{P}''_{n,m}(\cos\theta) = \left(\frac{2m^2}{1-\cos 2\theta} - n(n+1)\right)\bar{P}_{n,m} - \cot\theta\bar{P}'_{n,m}(\cos\theta) \tag{19}$$

5) Recurrence formula of $\bar{P}'''_{n,m}(\cos\theta)$

$$\bar{P}'''_{n,m}(\cos\theta) = -\frac{4m^2\cot\theta}{1-\cos 2\theta}\bar{P}_{n,m} - \cot\theta\bar{P}''_{n,m}(\cos\theta) + \left(\frac{2\left(1+m^2\right)}{1-\cos 2\theta} - n(n+1)\right)\bar{P}'_{n,m}(\cos\theta) \tag{20}$$

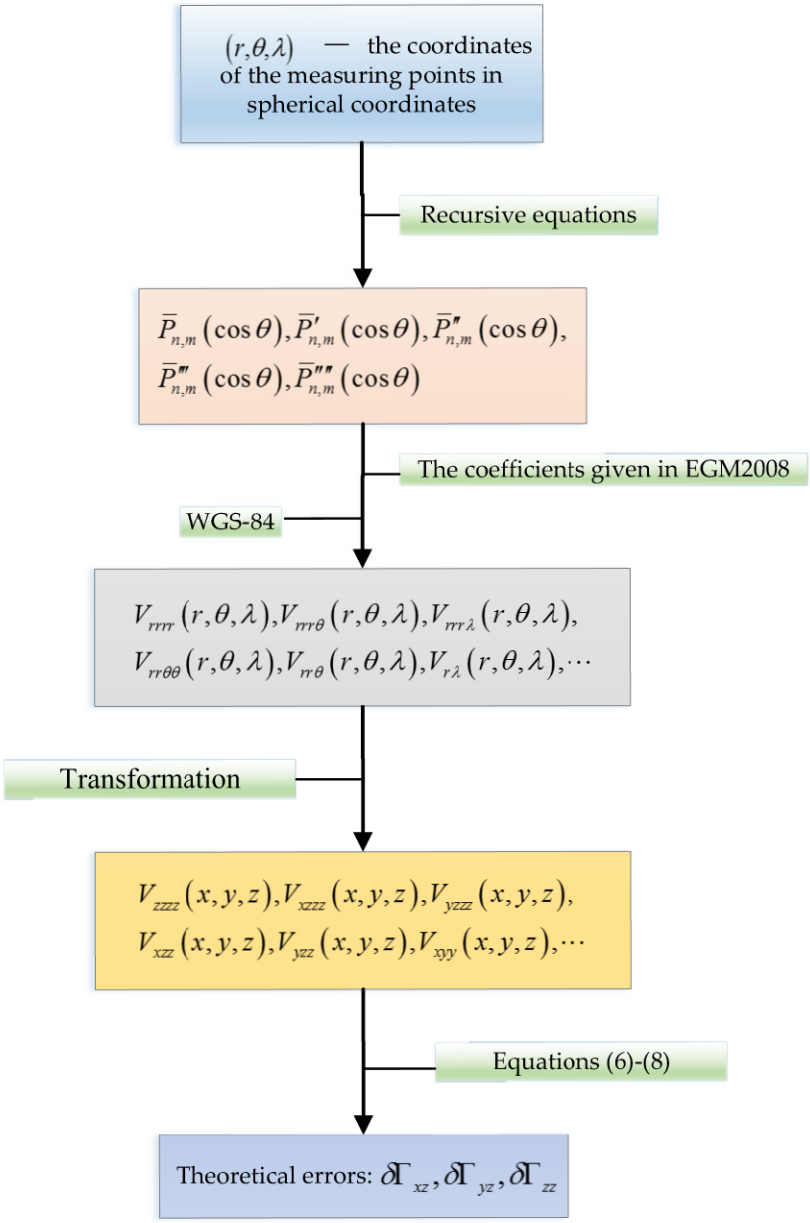

FIGURE 6. Flowchart of simulation experiment.

6) Recurrence formula of $\bar{P}''''_{n,m}(\cos\theta)$

$$\begin{aligned}\bar{P}''''_{n,m}(\cos\theta) &= 2m^2\left(\frac{2+6\cot^2\theta}{1-\cos 2\theta}\right)\bar{P}_{n,m}-\cot\theta\bar{P}'''_{n,m}(\cos\theta)\\ &-\left(\frac{4\left(1+2m^2\right)\cot\theta}{1-\cos 2\theta}\right)\bar{P}'_{n,m}(\cos\theta)\\ &+\left(\frac{2\left(2+m^2\right)}{1-\cos 2\theta}-n(n+1)\right)\bar{P}''_{n,m}(\cos\theta)\end{aligned}\tag{21}$$

The derivatives of the Legendre function can be calculated using Formulas (15)–(21).

IV. SIMULATION

In this section, we calculate the values of the omission errors in the gravity gradient measurement through a simulation experiment. The acceleration measurement devices are assumed to be capable of measuring the vertical component of gravity, and they are placed as shown in Figures 1 and 2. The distance between the acceleration measurement devices, namely, the baseline, is denoted by d.

TABLE 4. Mean values of omission errors in measuring gravity gradient component Γ_{xz}.

d (m)	A (Unit: E)		B (Unit: E)		C (Unit: E)	
	$\delta\Gamma_{xz}$	$\lvert\delta\Gamma_{xz}/\Gamma_{xz}\rvert$	$\delta\Gamma_{xz}$	$\lvert\delta\Gamma_{xz}/\Gamma_{xz}\rvert$	$\delta\Gamma_{xz}$	$\lvert\delta\Gamma_{xz}/\Gamma_{xz}\rvert$
0.4	1.3702999×10^{-5}	2.5094007×10^{-5}	-1.2176980×10^{-5}	1.3276331×10^{-6}	1.2294153×10^{-7}	1.2440918×10^{-8}
10	0.0114345	0.0209398	−0.0101608	0.0011078	1.0247790×10^{-4}	1.0370125×10^{-5}
100	1.1336495	2.0760279	−1.0079166	0.1098912	0.0123763	0.0012524

TABLE 5. Mean values of omission errors in measuring gravity gradient component Γ_{yz}.

d (m)	A (Unit: E)		B (Unit: E)		C (Unit: E)	
	$\delta\Gamma_{yz}$	$\lvert\delta\Gamma_{yz}/\Gamma_{yz}\rvert$	$\delta\Gamma_{yz}$	$\lvert\delta\Gamma_{yz}/\Gamma_{yz}\rvert$	$\delta\Gamma_{yz}$	$\lvert\delta\Gamma_{yz}/\Gamma_{yz}\rvert$
0.4	1.0930529×10^{-9}	3.4092902×10^{-9}	-2.3664836×10^{-7}	1.1111796×10^{-6}	1.9749213×10^{-7}	5.1137270×10^{-5}
10	9.1181930×10^{-7}	2.8440130×10^{-6}	-1.9746358×10^{-4}	9.2718793×10^{-4}	1.2436708×10^{-4}	0.0322028
100	9.0714561×10^{-5}	2.8294355×10^{-4}	−0.0195772	0.0919244	0.0122120	3.1621045

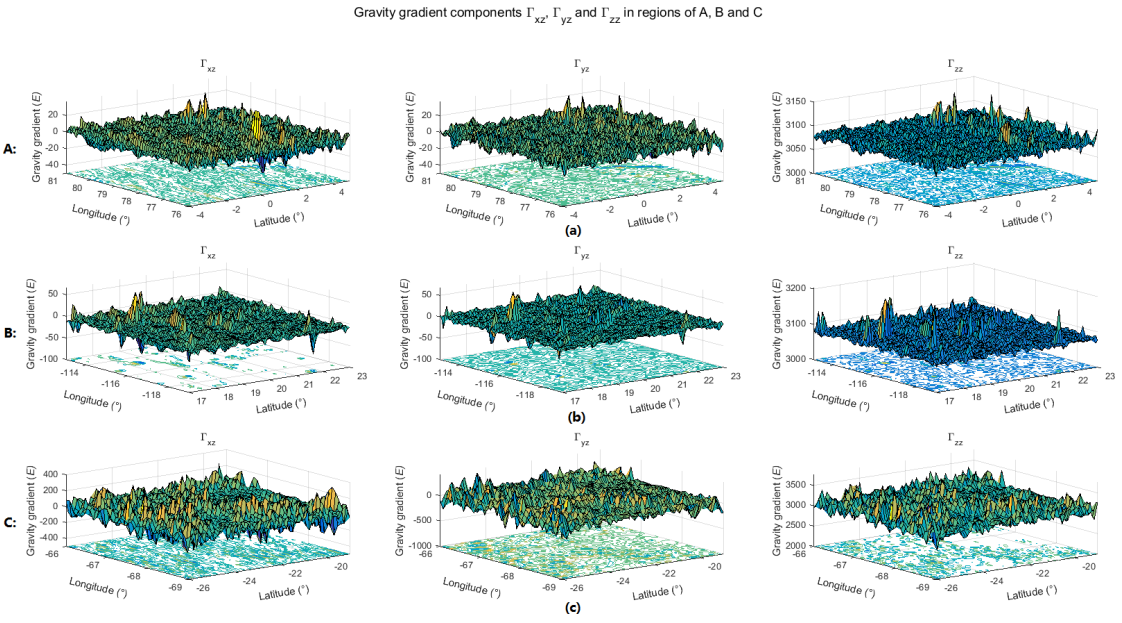

FIGURE 7. Gravity gradient components of three regions, calculated by EGM2008: values in (a) *A*, (b) *B*, and (c) *C*.

The measurement of the gravity gradient components Γ_{zz}, Γ_{xz} and Γ_{zz} can be achieved.

A. SIMULATION SETTINGS

The simulation conditions are shown in Table 1.

The baselines for different gravity gradient measurement devices vary. For example, for a rotating accelerometer gravity gradiometer (full-tensor gravity gradiometer, FTG), the baseline is approximately 0.2 m to 0.4 m; for the gravity gradient measurement developed by A. Araya and others, the baseline is approximately 0.44 m [34]; for the gravity gradient measurement in [28], the baseline is approximately 700 m. Therefore, the baselines in this study are set as 0.4, 10, and 100 m, to analyze the influences of omission errors in various measurement methods on the measurement results.

Although the spatial resolution of EGM2008 is approximately 10 km, which is much larger than the baseline length, EGM2008 can still be used to calculate the

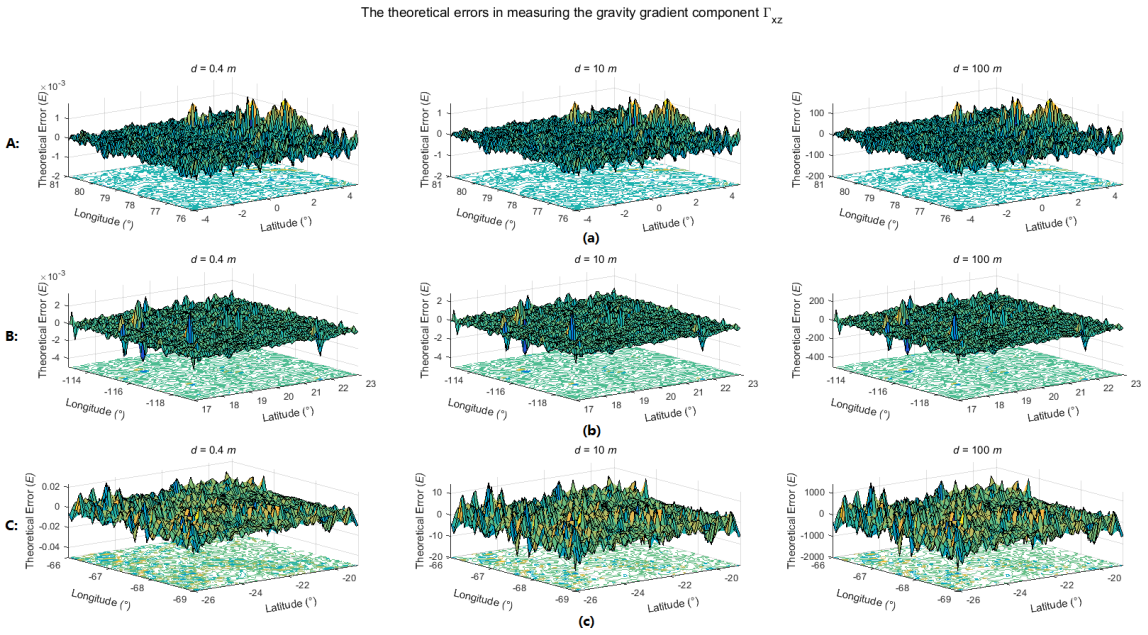

FIGURE 8. Omission errors in measuring gravity gradient component Γ_{xz} under various values of difference distance d in regions (a) *A*, (b) *B*, and (c) *C*.

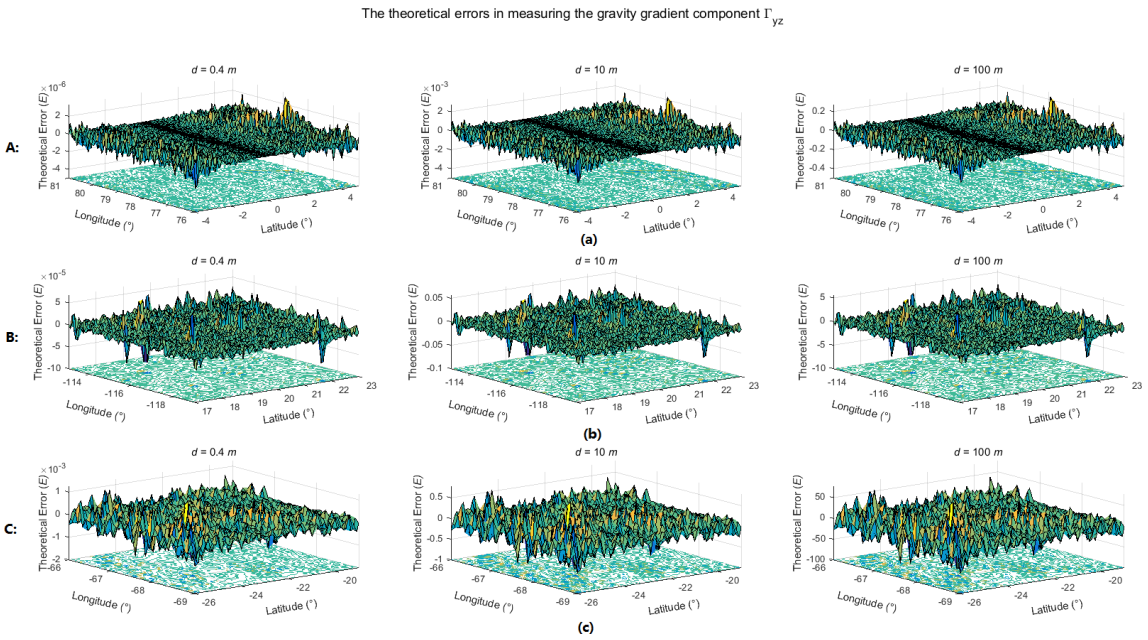

FIGURE 9. Omission errors in measuring gravity gradient component Γ_{yz} under various values of difference distance d in regions (a) *A*, (b) *B*, and (c) *C*.

omission errors in the simulation. The Appendix shows that the omitted high-order terms are closely related to the coordinates of the measuring points but are insignificantly correlated with the spatial resolution of the model.

Several regions are selected for the simulation to determine whether omission errors exert the same effects on the measurement results in different regions, which are shown in Figure 5. The regions in the red, yellow, and blue boxes are denoted as A, B, and C, respectively.

The latitude and longitude of each region are shown in Table 2. These regions are divided into $5' \times 5'$ grids in the simulation.

The simulation flowchart is shown in Figure 6. In the simulation, the omission errors of gravity gradient components Γ_{zz}, Γ_{xz} and Γ_{zz} are calculated. The reason for choosing these three components is because: on the one hand, the application of these three components is more extensive; on the other hand, the measurement of these components is relatively easy to operate in actual survey.

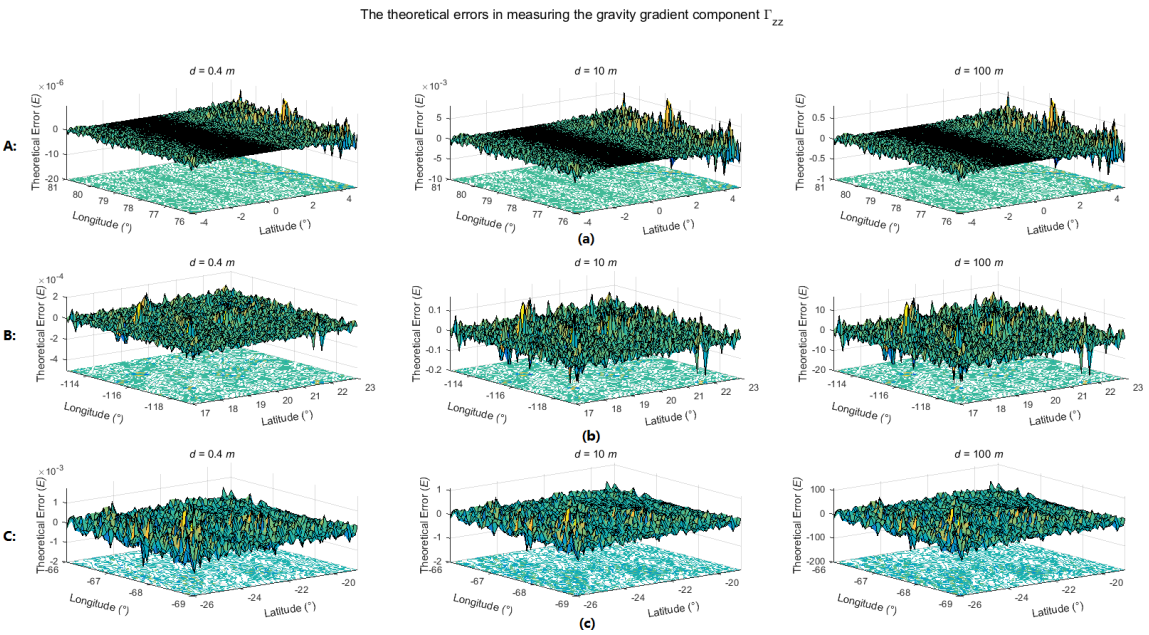

FIGURE 10. Omission errors in measuring gravity gradient component Γ_{zz} under various values of difference distance d in regions (a) A, (b) B, and (c) C.

TABLE 6. Mean values of omission errors in measuring gravity gradient component Γ_{zz}.

d (m)	A (Unit: E)		B (Unit: E)		C (Unit: E)	
	$\delta\Gamma_{zz}$	$\lvert\delta\Gamma_{zz}/\Gamma_{zz}\rvert$	$\delta\Gamma_{zz}$	$\lvert\delta\Gamma_{zz}/\Gamma_{zz}\rvert$	$\delta\Gamma_{zz}$	$\lvert\delta\Gamma_{zz}/\Gamma_{zz}\rvert$
0.4	-3.1051230×10^{-9}	1.0077049×10^{-12}	-2.2612071×10^{-8}	7.3364872×10^{-12}	5.9458959×10^{-8}	1.9271364×10^{-11}
10	-2.5935287×10^{-6}	8.4167731×10^{-10}	-1.8946991×10^{-5}	6.1473517×10^{-9}	3.7363289×10^{-5}	1.2109892×10^{-8}
100	-2.5630845×10^{-4}	8.3179726×10^{-8}	-0.0019341	6.2751545×10^{-7}	0.0038514	1.2482974×10^{-6}

B. SIMULATION RESULTS

The measurement environment and devices are assumed to be under ideal conditions in the simulation. The differential acceleration method is used to measure the gravity gradient components Γ_{xz}, Γ_{yz} and Γ_{zz}.

The values of the gravity gradient components of the three regions calculated by EGM2008 are shown in Figure 7, and the mean values of these components are shown in Table 3. These values are used as true values in the simulation.

The omission errors in measuring Γ_{xz}, Γ_{yz}, and Γ_{zz} are denoted by $\delta\Gamma_{xz}$, $\delta\Gamma_{yz}$, and $\delta\Gamma_{zz}$, respectively, and shown in Figures 8–10 and Tables 4–6.

V. DISCUSSION AND CONCLUSION

The omission errors of gravity gradient measurement based on differential acceleration are analyzed in this study. The values of several high-order terms in the gravity gradient measurement are calculated using EGM2008 and they are converted into the LNOF.

Previous works on gravity gradient measurement have considered that the omission of high-order terms does not affect the measurement results. However, limited analyses of omission errors exist in open literature. In this study, we show that the omission of high-order terms in short-baseline gravity gradient measurement insignificantly affects the measurement results. However, with an increase in baseline length, the omission errors increase and eventually affect the measurement results. When the baseline length is 100 m, the value of $|\delta\Gamma_{xz}/\Gamma_{xz}|$ in the region of A reaches 2.0760279 and the value of $|\delta\Gamma_{yz}/\Gamma_{yz}|$ in C reaches 3.1621045. Accordingly, when the baseline length d reaches 100 m, the gravity gradient components in certain regions will be submerged in omission errors and these gravity gradient components will not be measured.

Tables 4–6 present the following relationship between omission error and baseline length::

$$\left(\frac{\delta\Gamma_{iz}}{\delta\Gamma'_{iz}}\right) \approx \left(\frac{d}{d'}\right)^2 \quad (i \in \{x, y, z\}) \tag{22}$$

where $\delta\Gamma'_{iz}$ is the omission error before the change in d' and $\delta\Gamma_{iz}$ is the omission error after the change in baseline length.

The values of the omission errors can be estimated using Equation (22).

The influences of the omission errors on different regions also vary. When the baseline length is 100 m, as shown in Table 4, the relative error of the Γ_{xz} component in A is 2.0760279, which is greater than 1. By contrast, the relative errors of the Γ_{xz} component in the other regions are less than 1. Therefore, the Γ_{xz} component will be submerged in omission errors in A but not in B and C. A similar conclusion can be drawn from Table 5. The table shows that the relative error of the Γ_{yz} component in C is 3.1621045, whereas those of the Γ_{yz} component in the other regions are less than 1. The omission error thus has a greater influence on the gravitational gradient component Γ_{yz} in C than in A and B.

The component of Γ_{zz} is the least affected by omission error among the three components of Γ_{xz}, Γ_{yz}, and Γ_{zz}. A comparison of Tables 4–6 shows that the relative error of the component Γ_{zz} is the smallest in comparison with those of Γ_{xz}, Γ_{yz}, and Γ_{zz}, which means that the measured value of Γ_{zz} is the least affected by omission error. Therefore, the component of Γ_{zz} should be prioritized when using gravity gradient data.

In summary, from the results of this study, we can draw the following conclusions.

1) The error of omission of high-order terms is positively related to baseline length. For short-baseline (such as 0.4 m) gravity gradient measurements, the omission of high-order terms exerts a negligible effect on the measurement results. However, with an increase in baseline, the influence of omission error becomes increasingly large until the signals of gravity gradient components are drowned out by the omission error.
2) The influences of omission errors in different regions vary.
3) The component of Γ_{zz} should be prioritized when the data of gravity gradient measurement are applied.

APPENDIX

The expression for the omitted high-order terms in the EFRF is

$$\begin{aligned}&\frac{\partial^n g_i}{\partial r^{n_1}\partial\theta^{n_2}\partial\lambda^{n_3}}\\&=\frac{\partial^{n+1}V}{\partial r^{n_1}\partial\theta^{n_2}\partial\lambda^{n_3}\partial i}\\&=\frac{GM}{a}\sum_{n=0}^{N_{\max}}\gamma\left(\frac{a}{r}\right)^{n+1}\sum_{m=0}^{n}\left(\alpha\cos m\lambda+\beta\sin m\lambda\right)p\\&\quad\times\left(i\in\{r,\theta,\lambda\},n_1+n_2+n_3=n,n=1,2,3,\ldots\right)\end{aligned}\tag{A.1}$$

The parameters α, β, γ and p are shown in Table 7.

TABLE 7. Expressions of parameters α, β, γ, and p for high-order terms.

Terms	α	β	γ	p
V_{rrr}	$\bar{C}_{nm}$	$\bar{S}_{nm}$	$-\frac{(n+1)(n+2)(n+3)}{r^3}$	$\bar{P}_{nm}(\cos\theta)$
$V_{rr\theta}$	$\bar{C}_{nm}$	$\bar{S}_{nm}$	$\frac{(l+1)(l+2)}{r^2}$	$\bar{P}'_{nm}(\cos\theta)$
$V_{rr\lambda}$	$\bar{S}_{nm}$	$-\bar{C}_{nm}$	$\frac{(l+1)(l+2)}{r^2}$	$m\bar{P}_{nm}(\cos\theta)$
$V_{r\theta\theta}$	$\bar{C}_{nm}$	$\bar{S}_{nm}$	$-\frac{l+1}{r}$	$\bar{P}''_{nm}(\cos\theta)$
$V_{r\theta\lambda}$	$\bar{S}_{nm}$	$-\bar{C}_{nm}$	$-\frac{l+1}{r}$	$m\bar{P}'_{nm}(\cos\theta)$
$V_{r\lambda\lambda}$	$-\bar{C}_{nm}$	$-\bar{S}_{nm}$	$-\frac{l+1}{r}$	$m^2\bar{P}_{nm}(\cos\theta)$
$V_{\theta\theta\theta}$	$\bar{C}_{nm}$	$\bar{S}_{nm}$	1	$\bar{P}'''_{nm}(\cos\theta)$
$V_{\theta\theta\lambda}$	$\bar{S}_{nm}$	$-\bar{C}_{nm}$	1	$m\bar{P}''_{nm}(\cos\theta)$
$V_{\theta\lambda\lambda}$	$-\bar{C}_{nm}$	$-\bar{S}_{nm}$	1	$m^2\bar{P}'_{nm}(\cos\theta)$
$V_{\lambda\lambda\lambda}$	$-\bar{S}_{nm}$	$\bar{C}_{nm}$	1	$m^3\bar{P}_{nm}(\cos\theta)$
V_{rrr}	$\bar{C}_{lm}$	$\bar{S}_{lm}$	$\frac{(l+1)(l+2)(l+3)(l+4)}{r^4}$	$\bar{P}_{lm}(\cos\theta)$
$V_{rr\theta}$	$\bar{C}_{lm}$	$\bar{S}_{lm}$	$-\frac{(l+1)(l+2)(l+3)}{r^3}$	$\bar{P}'_{lm}(\cos\theta)$
$V_{rr\lambda}$	$\bar{S}_{lm}$	$-\bar{C}_{lm}$	$-\frac{(l+1)(l+2)(l+3)}{r^3}$	$m\bar{P}_{lm}(\cos\theta)$
$V_{r\theta\theta}$	$\bar{C}_{lm}$	$\bar{S}_{lm}$	$\frac{(l+1)(l+2)}{r^2}$	$\bar{P}''_{lm}(\cos\theta)$
$V_{r\theta\lambda}$	$\bar{S}_{lm}$	$-\bar{C}_{lm}$	$\frac{(l+1)(l+2)}{r^2}$	$m\bar{P}'_{lm}(\cos\theta)$
$V_{r\lambda\lambda}$	$-\bar{C}_{lm}$	$-\bar{S}_{lm}$	$\frac{(l+1)(l+2)}{r^2}$	$m^2\bar{P}_{lm}(\cos\theta)$
$V_{r\theta\theta}$	$\bar{C}_{lm}$	$\bar{S}_{lm}$	$-\frac{l+1}{r}$	$\bar{P}'''_{lm}(\cos\theta)$
$V_{r\theta\lambda}$	$\bar{S}_{lm}$	$-\bar{C}_{lm}$	$-\frac{l+1}{r}$	$m\bar{P}''_{lm}(\cos\theta)$
$V_{r\theta\lambda\lambda}$	$-\bar{C}_{lm}$	$-\bar{S}_{lm}$	$-\frac{l+1}{r}$	$m^2\bar{P}'_{lm}(\cos\theta)$
$V_{r\lambda\lambda\lambda}$	$-\bar{S}_{lm}$	$\bar{C}_{lm}$	$-\frac{l+1}{r}$	$m^3\bar{P}_{lm}(\cos\theta)$
$V_{\theta\theta\theta}$	$\bar{C}_{lm}$	$\bar{S}_{lm}$	1	$\bar{P}'''_{lm}(\cos\theta)$
$V_{\theta\theta\lambda}$	$\bar{S}_{lm}$	$-\bar{C}_{lm}$	1	$m\bar{P}''_{lm}(\cos\theta)$
$V_{\theta\lambda\lambda}$	$-\bar{C}_{lm}$	$-\bar{S}_{lm}$	1	$m^2\bar{P}''_{lm}(\cos\theta)$
$V_{\theta\lambda\lambda\lambda}$	$-\bar{S}_{lm}$	$\bar{C}_{lm}$	1	$m^3\bar{P}'_{lm}(\cos\theta)$
$V_{\lambda\lambda\lambda\lambda}$	$\bar{C}_{lm}$	$\bar{S}_{lm}$	1	$m^4\bar{P}_{lm}(\cos\theta)$

ACKNOWLEDGMENT

The authors would like to express our gratitude to all those who helped us during the writing of this paper.

REFERENCES

[1] J. Bouman *et al.*, "GOCE gravitational gradients along the orbit," *J. Geodesy*, vol. 85, p. 791, Nov. 2011.
[2] W. N. Zhou, Z. Y. Nan, and J. Y. Li, "Self-constrained euler deconvolution using potential field data of different altitudes," *Pure Appl. Geophys.*, vol. 173, no. 6, pp. 2073–2085, Jun. 2016.

[3] C. Jekeli, "Airborne gradiometry error analysis," *Surv. Geophys.*, vol. 27, no. 2, pp. 257–275, Mar. 2006.
[4] V. Mikhailov, G. Pajot, M. Diament, and A. Price, "Tensor deconvolution: A method to locate equivalent sources from full tensor gravity data," *Geophysics*, vol. 72, no. 5, pp. I61–I69, 2007.
[5] L. Wu and J. Tian, "Automated gravity gradient tensor inversion for underwater object detection," *J. Geophys. Eng.*, vol. 7, no. 4, pp. 410–416, 2010.
[6] K. Douch *et al.*, "Error analysis of a new planar electrostatic gravity gradiometer for airborne surveys," *J. Geodesy*, vol. 89, no. 12, pp. 1217–1231, 2015.
[7] K. Douch, B. Christophe, B. Foulon, I. Panet, G. Pajot-Métivier, and M. Diament, "Ultra-sensitive electrostatic planar acceleration gradiometer for airborne geophysical surveys," *Meas. Sci. Technol.*, vol. 25, no. 10, p. 105902, 2014.
[8] N. A. Lockerbie, "The location of subterranean voids using tensor gravity gradiometry," *Classical Quantum Gravity*, vol. 31, no. 6, p. 065011, 2014.
[9] X. C. Sun, P. Chen, C. Macabiau, and C. Hans, "A two-tiered approach to spacecraft positioning from significantly biased gravity gradient measurements," *Advances in the Astronautical Sciences Astrodynamics*, M. Majji, J. D. Turner, G. G. Wawrzyniak, and W. T. Cerven, Eds. San Diego, CA, USA: Univelt, 2016, pp. 1853–1868.
[10] F. M. Liu, D. Qian, F. M. Liu, and Y. Li, "Integrated navigation system based on correlation between gravity gradient and terrain," in *Proc. Int. Joint Conf. Comput. Sci. Optim. (CSO)*, Los Alamitos, CA, USA, Apr. 2009, pp. 289–293.
[11] L. Xiong, J. Ma, L. Zhang, J. W. Tian, and J. Liu, "Submarine navigation based on gravity gradient-terrain matching," in *Proc. SPIE*, Wuhan, China, 2007, pp. S7904–S7904.
[12] C. Jekeli, "Precision free-inertial navigation with gravity compensation by an onboard gradiometer," *J. Guid., Control, Dyn.*, vol. 29, no. 3, pp. 704–713, 2006.
[13] J. Lee, J. H. Kwon, and M. Yu, "Performance evaluation and requirements assessment for gravity gradient referenced navigation," *Sensors*, vol. 15, no. 7, pp. 16833–16847, 2015.
[14] X. C. Sun, P. Chen, C. Macabiau, and C. Han, "Low-earth orbit determination from gravity gradient measurements," *Acta Astronautica*, vol. 123, pp. 350–362, Jun./Jul. 2016.
[15] S. Yan, Y. Xie, M. Zhang, Z. Deng, and L. Tu, "A subnano-g electrostatic force-rebalanced flexure accelerometer for gravity gradient instruments," *Sensors*, vol. 17, no. 11, p.E2669, 2017.
[16] X. Huang, Z. Deng, Y. Xie, Z. Li, J. Fan, and L. Tu, "A new scale factor adjustment method for magnetic force feedback accelerometer," *Sensors*, vol. 17, no. 11, p. E2471, 2017.
[17] M. J. Fuchs and J. Bouman, "Rotation of GOCE gravity gradients to local frames," *Geophys. J. Int.*, vol. 187, no. 2, pp. 743–753, 2011.
[18] R. Pail, "A parametric study on the impact of satellite attitude errors on GOCE gravity field recovery," *J. Geodesy*, vol. 79, nos. 4–5, pp. 231–241, Jul. 2005.
[19] X.-Q. Li, M.-X. Shao, H. J. Paik, Y.-C. Huang, T.-X. Song, and X. Bian, "Effects of satellite positioning errors and EarthŠs multipole moments in the detection of the gravitomagnetic field with an orbiting gravity gradiometer," *Gen. Relativity Gravitation*, vol. 46, p. 1737, May 2014.
[20] J. Bouman, R. Koop, C. C. Tscherning, and P. Visser, "Calibration of GOCE SGG data using high–low SST, terrestrial gravity data and global gravity field models," *J. Geodesy*, vol. 78, nos. 1–2, pp. 124–137, 2004.
[21] Y.-P. Wang *et al.*, "Extracting the differential phase in dual atom interferometers by modulating magnetic fields," *Opt. Commun.*, vol. 375, pp. 34–37, Sep. 2016.
[22] S. Rispens and J. Bouman, "Calibrating the GOCE accelerations with star sensor data and a global gravity field model," *J. Geodesy*, vol. 83, no. 8, pp. 737–749, 2009.
[23] J. Bouman *et al.*, "Preprocessing of gravity gradients at the GOCE high-level processing facility," *J. Geodesy*, vol. 83, no. 7, pp. 659–678, 2009.
[24] M. V. Moody, H. J. Paik, and E. R. Canavan, "Three-axis superconducting gravity gradiometer for sensitive gravity experiments," *Rev. Sci. Instrum.*, vol. 73, no. 11, pp. 3957–3974, Nov. 2002.
[25] J. M. McGuirk, G. T. Foster, J. B. Fixler, M. J. Snadden, and M. A. Kasevich, "Sensitive absolute-gravity gradiometry using atom interferometry," *Phys. Rev. A, Gen. Phys.*, vol. 65, no. 3, p. 033608, 2002.
[26] A. Araya *et al.*, "Gravity gradiometer implemented in AUV for detection of seafloor massive sulfides," in *Proc. OCEANS*. New York, NY, USA: IEEE, Oct. 2012, pp. 1–4.
[27] C. Jekeli, "A wavelet approach to the terrain correction in gravimetry and gravity gradiometry," *GEM-Int. J. Geomathematics*, vol. 3, no. 1, pp. 139–154, 2012.
[28] L. K. Zheleznyak, V. N. Koneshov, and P. S. Mikhailov, "Experimental determination of the vertical gravity gradient below the sea level," *Izvestiya-Phys. Solid Earth*, vol. 52, no. 6, pp. 866–868, 2016.
[29] W. A. Heiskanen and H. Moritz, "The gravity field of the earth," in *Physical Geodesy*. San Francisco, CA, USA: Freeman, 1967, pp. 47–48.
[30] N. K. Pavlis, S. A. Holmes, S. C. Kenyon, and J. K. Factor, "An earth gravitational model to degree 2160: EGM2008," in *Proc. Gen. Assem. EGU*, Vienna, Austria, 2008, p. 1.
[31] N. K. Pavlis, S. A. Holmes, S. C. Kenyon, and J. K. Factor, "The development and evaluation of the earth gravitational model 2008 (EGM2008)," *J. Geophys. Res.-Solid Earth*, vol. 118, no. 5, pp. 2633–2633, May 2013.
[32] D. H. Titterton and J. L. Weston, *Strapdown Inertial Navigation Technology*. London, U.K.: Institution of Electrical Engineers, 2004, pp. 21–22.
[33] Y. Su, D. Fan, and W. You, "Fast and stably recursive algorithm for computing second derivative of associated legendre functions," *Geomatics Inf. Sci. Wuhan Univ.*, vol. 37, no. 12, pp. 1409–1412, Dec. 2012.
[34] A. Araya *et al.*, "Development and demonstration of a gravity gradiometer onboard an autonomous underwater vehicle for detecting massive subseafloor deposits," *Ocean Eng.*, vol. 105, pp. 64–71, Sep. 2015.

HONGWEI WEI received the B.S. degree in automation from Harbin Engineering University, Harbin, China, in 2011, and the M.S. degree in control science and engineering from the College of Mechatronic Engineering and Automation, National University of Defense Technology, Changsha, China, in 2013, where he is currently pursuing the Ph.D. degree. His research interests include gravity and gravity gradient measurement.

MEIPING WU received the Ph.D. degree in control science and engineering from the National University of Defense Technology, Changsha, China, in 2000. He is currently a Professor with the Department of Automatic Control, National University of Defense Technology. His research interests include inertial navigation technology, gravity modeling, gravity measurement, and gravity gradient measurement.

JULIANG CAO received the Ph.D. degree in control science and engineering from the National University of Defense Technology, Changsha, China, in 2004. He is currently a Professor with the Department of Automatic Control, National University of Defense Technology. His research interests include inertial navigation technology, underwater gravity measurement, and circuit design.

JUNXIANG LIAN received the Ph.D. degree in control science and engineering from the National University of Defense Technology, Changsha, China, in 2007. He is currently an Associate Professor with the Department of Automatic Control, National University of Defense Technology. His research interests include bionic navigation, polarized light navigation, and gravity assisted navigation.

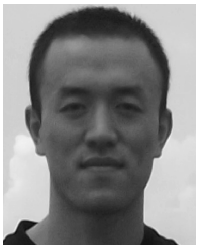

SHAOKUN CAI received the Ph.D. degree in control science and engineering from the National University of Defense Technology, Changsha, China, in 2014. He is currently a Lecturer with the Department of Automatic Control, National University of Defense Technology. His research interests include inertial navigation technology and airborne gravity vector measurement.